

# Study of the Process of Leaching of Long-Lived Radionuclides $^{14}\text{C}$ and $^{36}\text{Cl}$ from Irradiated Graphite

A. O. Pavlyuk<sup>a</sup>, S. G. Kotlyarevskii<sup>a</sup>, R. I. Kan<sup>a</sup>, A. G. Volkova<sup>b,\*</sup>, and E. V. Zakharova<sup>b</sup>

<sup>a</sup> Pilot and Demonstration Center for Decommissioning of Uranium-Graphite Nuclear Reactors, Seversk, Tomsk oblast, 636000 Russia

<sup>b</sup> Frumkin Institute of Physical Chemistry and Electrochemistry, Russian Academy of Sciences, Moscow, 119071 Russia

\*e-mail: anna.agv@yandex.ru

Received December 16, 2019; revised September 9, 2020; accepted September 15, 2020

**Abstract**—The release of long-lived radionuclides  $^{14}\text{C}$  and  $^{36}\text{Cl}$ , which are key products for assessment of disposal variants (near-surface, buried, or deep) of irradiated graphite, was analyzed. Test material was irradiated graphite from IUGR and RBMK-1000 reactors. Unlike other types of radioactive waste (RAW), graphite has the developed pore structure and, consequently, its effective surface area in contact with the leaching medium is increased in comparison with non-porous materials. With due regard for the graphite pore structure, the mechanism describing the leaching process is proposed and experimentally substantiated. The parameters numerically characterizing graphite RAW in terms of leaching resistance, independent of the geometric shape of individual fragments (samples) are also introduced. The proposed parameters and an algorithm for their determination are recommended by the authors for use in predictive calculations of the release of radionuclides from graphite under conditions of long-term storage/disposal.

**Keywords:** irradiated graphite, pore structure, long-lived radionuclides, leaching of radionuclides, radioactive waste

**DOI:** 10.1134/S1066362221020090

## INTRODUCTION

At present, the Russian Federation has accumulated about 60 thousand tons of irradiated graphite. Various approaches to handling graphite RAW are considered [1].

RAW in the form of irradiated graphite is: graphite blocks of reactor masonry, replaceable graphite parts (bushings, rings, and displacers), and fragments, chips, and other residuals formed in processing of parts of graphite masonry [2–6].

The degree of potential hazard of the bulk of graphite RAW (~95%) is determined by the presence of predominantly long-lived radionuclides (LLN)  $^{14}\text{C}$  and  $^{36}\text{Cl}$  [1].

Results of studies [4, 6] on the accumulation and distribution of radionuclides in irradiated graphite show that a complex pattern of radionuclide contamination is formed in graphite during the operation of the reactor. Its formation is influenced by both the operation conditions and the structural peculiarities of graphite itself, in particular by the pore structure characteristics, such as the volume of open porosity, the set of interconnected pore

channels, the distribution of pores along the radii of the maximum flow area, and others.

To justify any of the approaches, it is necessary to perform predictive safety assessments of their temporary storage or disposal. The key initial data for predictive assessments of the radiological hazard of disposal of various types of graphite waste will be: specific activity of long-lived nuclides and parameters characterizing the leaching of long-lived nuclides from graphite radioactive waste.

In this study, the processes of leaching of  $^{14}\text{C}$  and  $^{36}\text{Cl}$  from irradiated graphite were analyzed, depending on the brand of graphite, the type of parts, and the shape and size of the samples. The parameters characterizing the leaching of  $^{14}\text{C}$  and  $^{36}\text{Cl}$  from disposed waste were determined.

## EXPERIMENTAL

**Analysis of the influence of the pore structure of irradiated graphite on the leaching of main long-lived radionuclides from graphite RAW. GOSTs**

(State Standards) [7, 8] traditionally used in the Russian Federation for determination of leaching rate have been developed for solidified RAW and are based on the following basic principles:

– Test material is homogeneous, monolithic, and interacts with the leaching solution only on the surface of the sample;

– According to GOST, the final result is determination of leaching rate on time dependence, with the open surface area of monolithic sample taken into account in calculations [Eq. (1)].

$$R_n^i = \frac{a_n^i}{A^i F_0 t_n}, \quad (1)$$

where  $R_n^i$  is the rate of leaching of  $i$ th radionuclide during  $n$ th leaching period, related to the geometric surface area of a sample or fragment,  $\text{g}/(\text{cm}^2 \text{ day})$ ;  $a_n^i$  is the activity of  $i$ th radionuclide that passed into solution during the  $n$ th period of leaching, Bq;  $A^i$  is the specific activity of  $i$ th radionuclide in graphite,  $\text{Bq}/\text{g}$ ;  $F_0$  is the geometric surface area of a sample or fragment,  $\text{cm}^2$ ; and  $t_n$  is the duration of  $n$ th period of leaching, day.

In a study [9], model was proposed for describing the leaching process of the main long-lived radionuclides ( $^{14}\text{C}$  and  $^{36}\text{Cl}$ ) from irradiated graphite, taking into account the pore structure of graphite (namely, a developed system of open pores), as well as the peculiarities of the formation, retention, and distribution of  $^{14}\text{C}$  and  $^{36}\text{Cl}$  in the graphite structure. According to the proposed model, the leaching of  $^{14}\text{C}$  and  $^{36}\text{Cl}$  from irradiated graphite can be described by the following mechanism: after the filling of all accessible cavities in the graphite structure (pores, etc.) with a contact solution is complete, the effective leaching surface area and the intensity of mass exchange of the leaching solution stabilize. The intensity of sorption/desorption of radionuclides also comes to equilibrium during their migration along the pore channels to the sample surface. Further, the dynamics of the leaching process begins to be monotonic with a tendency for a slow decrease in intensity, the value of which will be determined by retention strength of radionuclides (their physicochemical forms) in the near-surface layers throughout the effective surface area in contact with a leaching solution and time delay due to the transport of radionuclides along the pores from the deep regions of the sample to its surface.

For stable leaching process, the effective leaching surface area is determined by Eq. (2):

$$F_{\text{eff}} = F_0 + F_S, \quad (2)$$

where  $F_{\text{eff}}$  is the effective leaching surface area of a sample,  $\text{cm}^2$ ;  $F_0$  is its geometric surface area,  $\text{cm}^2$ ; and  $F_S$  is the surface area accessible to the solution (open pores, intercrystallite spaces, etc.),  $\text{cm}^2$ .

In this case, the resistance of graphite RAW will be characterized by the leaching rate of a long-lived radionuclide, related to the effective leaching surface area, i.e., by the effective leaching rate  $R_{\text{eff}}$ .  $R_{\text{eff}}$  is determined by Eq. (3):

$$R_{\text{eff}}^i = \frac{a_n^i}{A^i (F_0 + F_S) t_n}, \quad (3)$$

where  $R_{\text{eff}}^i$  is the leaching rate of  $i$ th radionuclide during  $n$ th leaching period, related to the effective leaching surface area,  $\text{g}/(\text{cm}^2 \text{ day})$ .

Study of the pore structure of graphite of domestic brands (GR-76, GR-220, and GR-280) showed that almost the whole volume of open porosity in both virgin and irradiated graphite is accessible for saturation with water when kept in an aqueous medium [9]. During the operation in the reactor, the fraction of open porosity has tendency to a slight decrease. The surface area of open pores in graphite of the studied brands, even in the case of small graphite volumes, significantly (more than 2 orders of magnitude) exceeds the surface area of graphite fragments. Therefore, the leaching process of the main volumetrically distributed long-lived radionuclides has close to a “volume” character. In this case, the contribution of open pores to the leaching intensity will dominate over the contribution of the outer surface of the fragments.

Assuming that the whole volume of open pores (or most of it) in the sample is filled with a leaching solution and  $F_S \gg F_0$ , Eq. (3) can be written as:

$$R_{\text{eff}}^i = \frac{a_n^i}{A^i F_S t_n}, \quad (4)$$

If assessible pores are filled with a leaching solution in the volume of the sample,  $R_{\text{eff}}$  will not depend on its geometry and will determine the true resistance to leaching of  $^{14}\text{C}$  and  $^{36}\text{Cl}$  present in irradiated graphite, taking into account: spatial distribution of radionuclides in the graphite structure and retention strength of

radionuclides (their compounds) in graphite and their ability to form water-soluble compounds.

Considering pore structure of graphite as a network of interconnected channels with a circular cross section allows estimation of their surface area from the equation:

$$F_s = \frac{2vV}{r},$$

where  $v$  is volume fraction of open pores in graphite,  $V$  is the volume of a sample,  $\text{cm}^3$ , and  $r$ , the average cross section radius of open pores,  $\text{cm}$ .

If the accessible pores are equally filled with a solution throughout the volume of the sample, Eq. (4) can be written as:

$$R_{\text{eff}n}^i = \frac{a_n^i}{A^i k V t_n} = \frac{a_n^i \rho}{A^i k m t_n}, \quad (5)$$

where  $\rho$  is graphie density,  $\text{g}/\text{cm}^3$ , and  $m$ , sample mass.

From Eq. (1), the coefficient  $k$  has the form:

$$k = \frac{2v}{r},$$

where  $k$  is the proportionality coefficient, which depends on the volume fraction of pores and the distribution of pores accessible to a leaching solution over their diameter (or average diameter),  $\text{cm}^{-1}$ ;  $v$  is the volume fraction of open pores in graphite;  $r$  is the average cross section radius of open pores,  $\text{cm}$ .

The equation (5) can be also written as follows:

$$R_{\text{eff}n}^i = \gamma_n^i \frac{\rho}{k} = \gamma_n^i \frac{\rho r}{2v}, \quad (6)$$

where  $\gamma_n^i$  is determined by the expression:

$$\gamma_n^i = \frac{a_n^i}{A^i m t_n} = \frac{a_n^i}{A^i \rho V t_n}, \quad (7)$$

The physical meaning of  $\gamma_n^i$  is the fraction of the  $i$ th radionuclide released from the material of the sample per unit time during the  $n$ th leaching period,  $\text{day}^{-1}$  (or  $100 \gamma_n^i, \% / \text{day}$ ).

It should be noted that Eqs. (4)–(6) are valid at the following conditions: the filling of all accessible cavities in the graphite structure (pores, intercrystallite spaces, etc.) with a contact solution has stopped, and, consequently,

the effective leaching surface area and the intensity of mass exchange between the leaching solution in the pore volume and that in the external volume are stabilized;  $F_s \gg F_0$ ; pores are filled with a solution throughout the volume of the sample, the value of  $k$  is constant in the volume of the sample (fragment) and does not depend on the distance to the “sample-solution” interface; the intensity of sorption / desorption of radionuclides during the migration along the pore channels to the surface of the fragment attained equilibrium.

Note,  $R_{\text{eff}n}^i$  is directly proportional to  $\gamma_n^i$  (Eqs. 6 and 7), the proportionality coefficient  $\rho/k$  in Eq. (6) is determined solely by the graphite properties and does not depend on the sample geometry. Consequently, the parameter  $\gamma_n^i$ , as well as  $R_{\text{eff}n}^i$ , does not depend on the sample geometry and characterizes the studied material in terms of resistance to leaching of  $^{14}\text{C}$  and  $^{36}\text{Cl}$ .

## RESULTS AND DISCUSSION

**Experimental results on the release of long-lived radionuclides  $^{14}\text{C}$  and  $^{36}\text{Cl}$  from irradiated graphite during the leaching.** To verify the applicability of the model proposed in a study [9] for describing the mechanism of leaching of  $^{14}\text{C}$  and  $^{36}\text{Cl}$ , three series of experiments were performed. In the first series 1.5 years long, we studied samples of graphite parts of the same type from IUGR, irradiated in the reactor under the same conditions (duration, neutron flux, and temperature), whereas significantly different in geometric characteristics: one sample was with a volume within  $1 \text{ cm}^3$  and two samples were with a volume of up to  $450 \text{ cm}^3$  (Table 1, Fig. 1).

The tests were performed by keeping the samples in a contact fluid (distilled water) at a temperature of  $22\text{--}25^\circ\text{C}$ . During exposure, the solution was replaced and sampled after a certain period of time, and the content of  $^{14}\text{C}$  and  $^{36}\text{Cl}$  was determined. The results of the analyses were used to calculate  $R_n^i$  and  $\gamma_n^i$  from Eqs. (1) and (7), respectively.

Figures 2, 3 show run of the dependences of the leaching parameters  $R_n^i$  and  $\gamma_n^i$  on time  $t$  in the period after the stabilization of the process was attained ( $t > 50$  days).

It should be emphasized that test samples were made of graphite of the same brand, operated in the reactor under the same conditions, and contain virtually the same amount of  $^{14}\text{C}$  and  $^{36}\text{Cl}$  (Table 1). Thus, if the release of radionuclides into water was due only to leaching from the

**Table 1.** Characteristics of samples of GR-76 irradiated graphite for leaching tests

| Sample     | Part, graphite brand     | Shape and size of samples   | Irradiation time, year | Specific activity of $^{14}\text{C}$ , Bq/g | Specific activity of $^{36}\text{Cl}$ , Bq/g |
|------------|--------------------------|---|------------------------|---|--|
| Type 1     | Graphite bushings, GR-76 | Cylindrical shape:<br>$d \sim 8$ mm, $h \sim 10$ mm,<br>$V/F_0 \sim 0.14$   | 2.5                    | $1.35 \times 10^5$                          | 63   |
| Types 2, 3 | Graphite bushing, GR-76  | Fragments of graphite bushing:<br>$D_{\text{out}} \sim 86$ mm, $d_{\text{in}} \sim 46$ mm.<br>Type 2: $h \sim 60$ mm,<br>$V/F_0 \sim 0.62$ .<br>Type 3: $h \sim 109.5$ mm,<br>$V/F_0 \sim 0.72$ . | 2.5                    | $1.31 \times 10^{5a}$                       | 83 <sup>a</sup>                              |

<sup>a</sup> Average value by volume of graphite bushing for sample types 2 and 3.

sample surface and the leaching area was determined by the surface area of the sample, then all the  $R_n^i(t)$  curves would have to coincide. In this case, the fraction of  $^{14}\text{C}$  and  $^{36}\text{Cl}$  leached per unit time and the  $\gamma_n^i(t)$  curve for large fragments (type 2 and 3) would run significantly lower than those for small samples (type 1) due to the larger  $V/F_0$  ratio (0.62 and 0.72 cm for types 2 and 3, respectively, compared to 0.14 cm for type 1).

However, test results show that, with practically the same irradiation conditions (duration and temperature) and the same samples' characteristics (specific activity), the  $R_n^i(t)$  curves for samples of type 2 and 3 (large bushing fragments) lie higher than those for type 1 samples (small samples): by almost an order of magnitude higher for  $^{14}\text{C}$  and 5–7-fold higher for  $^{36}\text{Cl}$  (Figs. 2, 3). For samples of types 2 and 3, though  $\sim 2$  times different in lengths, the  $R_n^i(t)$  curves virtually coincide, since the  $V/F_0$  ratios for them are close. In this case, the  $\gamma_n^i$  values and the  $\gamma_n^i(t)$  curves for large fragments (types 2 and 3) and small

samples (type 1) with respect to both radionuclides,  $^{14}\text{C}$  and  $^{36}\text{Cl}$ , virtually coincide. Thus, the geometric shape and dimensions of test samples practically do not affect the parameter  $\gamma_n^i$ , characterizing the leaching resistance of a material, which is possible, if test samples are made of the same material and the leaching process has a volume rather than surface character.

For graphite, this leaching character is due to a developed system of pores accessible for leaching in the bulk of the sample when their leaching surface area is significantly larger than the geometric surface area of the sample. Since the pore network is a set of interconnected channels [9], only the time of saturation of the pores and the delay time of radionuclide release into the solution, determined by the mass-exchange rate of the leaching solution, will depend on the sample size.

In the second series of experiments, the leaching of  $^{14}\text{C}$  and  $^{36}\text{Cl}$  from two brands of graphite with different irradiation history was determined: two samples from a graphite bushing (brand GR-76) were irradiated for 2.5 years and two samples from a graphite block (brand GR-220) were irradiated for 34 years. The tests were performed by keeping the samples in distilled water for 1.5 years. In the course of the exposure, the contact fluid was replaced and sampled after certain intervals of time, and the  $^{14}\text{C}$  and  $^{36}\text{Cl}$  content was determined

To assess the resistance to leaching, the same parameter,  $R_n^i(t)$ , was determined as in the previous experiment.  $R_n^i(t)$  and  $\gamma_n^i(t)$  relate as:

$$R_n^i = \gamma_n^i \frac{m}{F_0} = \gamma_n^i \rho \frac{V}{F_0} \quad (8)$$

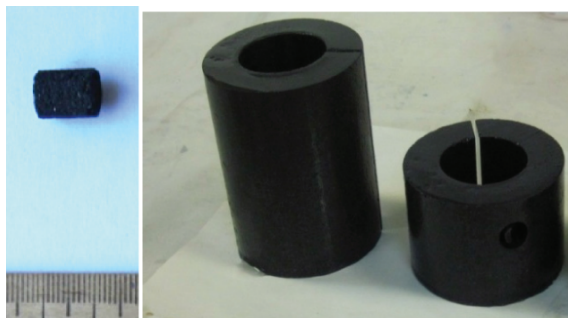


**Fig. 1.** Samples of irradiated graphite of GR-76 brand for leaching tests: type 1 (a), and types 2, 3 (b).

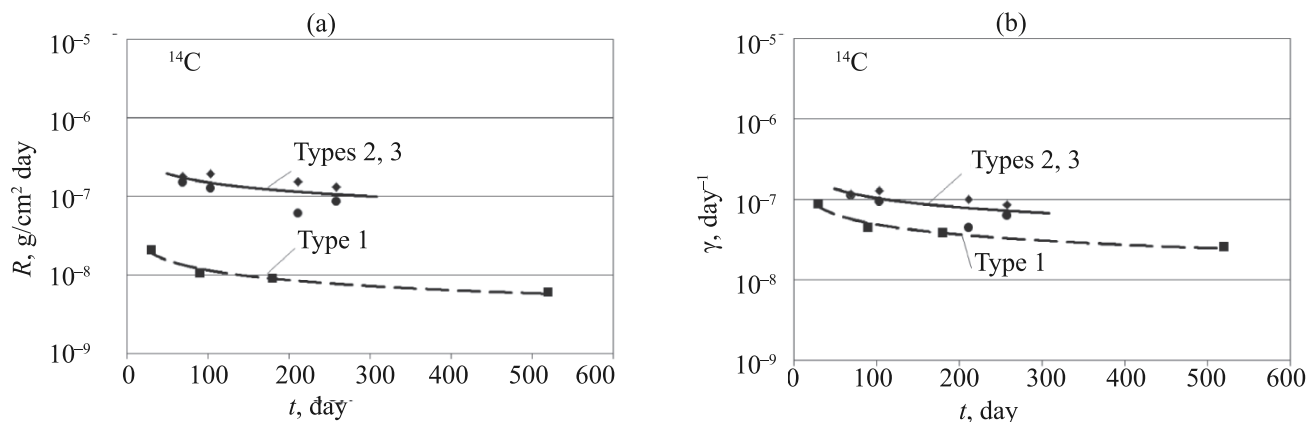


**Fig. 2.** Change in the leaching parameters of  $^{14}\text{C}$  from GR-76 irradiated graphite with time for samples of types 1, 2, and 3: (a) the rate of leaching of the  $i$ th radionuclide,  $R_n^i$ , and (b) fraction of leached  $i$ th radionuclide,  $\gamma_n^i$ .

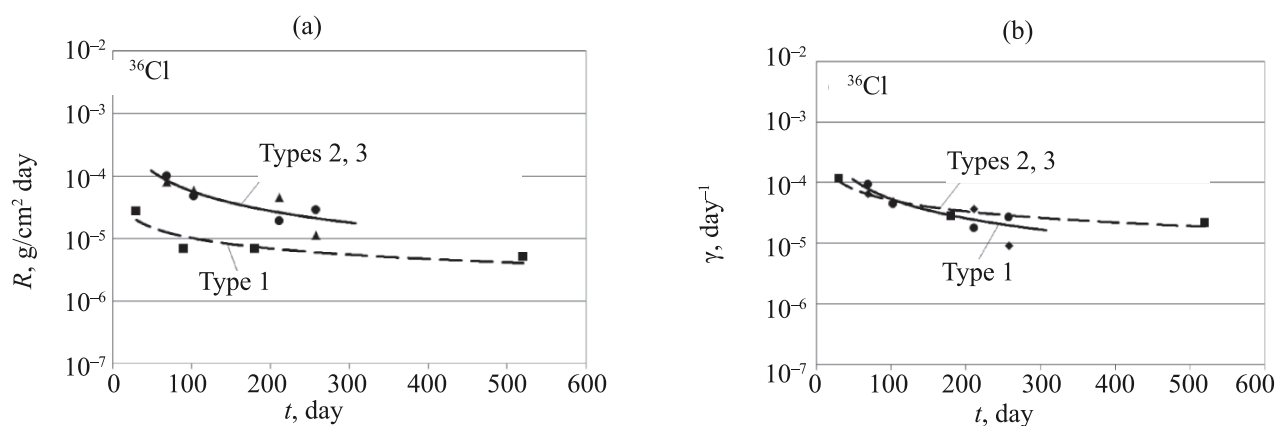


**Fig. 3.** Change in the leaching parameters of  $^{36}\text{Cl}$  from GR-76 irradiated graphite with time for samples of types 1, 2, and 3: (a) the rate of leaching of the  $i$ th radionuclide,  $R_n^i$ , and (b) fraction of leached  $i$ th radionuclide,  $\gamma_n^i$ .

Since the geometry of the samples is identical, in the case of the same resistance to leaching for both types of the samples, the  $R_n^i$  values should be the same.

However, the results showed a significant difference between the tested materials in terms of resistance to leaching of these isotopes (Fig. 4). Due to the identity of the geometry, the same differences between the curves of leaching dynamics for graphite of both brands characterize the dynamics of the parameter  $\gamma_n^i(t)$ , since, as follows from Eq. (8), in the given case, the relation  $R_n^i/\gamma_n^i = \text{const}$  is valid for each brand of graphite with respect to each isotope.

Evidently, the leaching dependences for  $^{14}\text{C}$  and  $^{36}\text{Cl}$  have the same character. In the initial period of interaction with the contact solution ( $t < 50\text{--}150$  days), the leaching rate decreases sharply (by  $10^2\text{--}10^3$  times).

Then, it continues to decrease, whereas significantly slower. This result can be explained by the fact that during the initial period of exposure, the process of filling all accessible cavities in the graphite structure (pores, intercrystallite spaces, etc.) with the contact solution stopped, thereby the value of the effective leaching surface area stabilized, and the intensity of sorption/desorption of radionuclides in the course of migration along the pore channels to the surface of the fragment attained equilibrium. Further, the intensity of the process is determined by:

- the retention strength of radionuclides (their physical and chemical forms) in the near-surface layers throughout the effective surface area in contact with the solution;
- the rate of mass exchange of the contact solution in the structural cavities in the graphite volume with the solution above the surface of a sample.

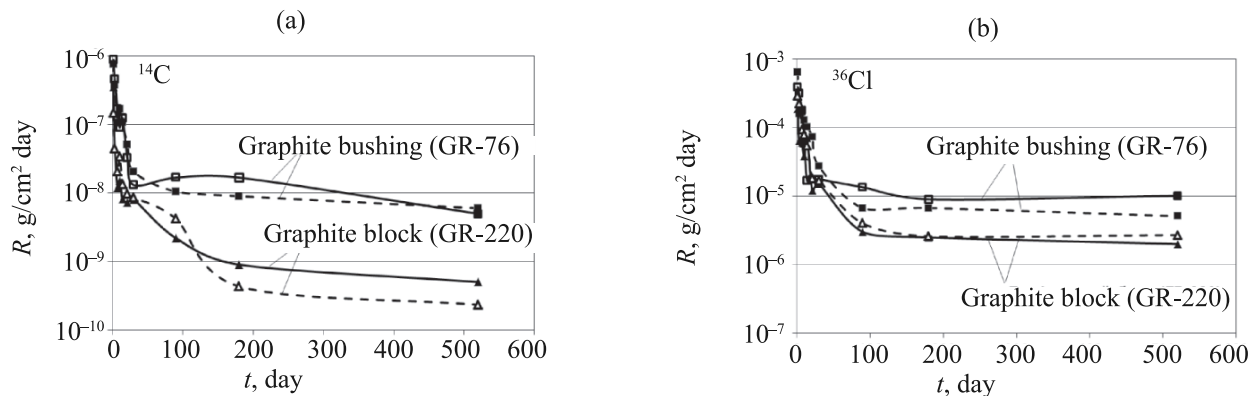


**Fig. 4.** Dynamics of the leaching rate of (a) <sup>14</sup>C and (b) <sup>36</sup>Cl from samples of the same geometry made of different brands of graphite (two samples of GR-76 bushing graphite and two samples of GR-220 block graphite).

Experimental curves in Fig. 4 demonstrate difference in the leaching intensity of <sup>14</sup>C and <sup>36</sup>Cl between GR-76 bushing and GR-220 block graphites. In relation to both radionuclides, the most resistant to leaching is graphite GR-220. The leaching rate parameter is lower in comparison with GR-76 by ~10–15 times for <sup>14</sup>C and ~3–5 times for <sup>36</sup>Cl. This result cannot be explained by difference in the effective leaching surface areas, determined mainly by the surface area of open pores. The results on study of the porosity of these brands of graphite (including irradiated graphite) showed that the fraction of open pore volume for these brands of irradiated graphite can spread in values within 20%, and the average radii of the pore throat cross sections have practically no statistically significant differences [9].

Most likely, the above differences in Fig. 4 are explained by: difference in the retention strength of radionuclides in bush and block graphite owing to different irradiation temperatures and peculiarities related to the mechanisms of formation, retention, and spatial distribution of these nuclides in graphite [10–16].

The irradiation temperature of the samples of block graphite exceeded that of the bushings by 200–300°C. Due to the higher irradiation temperature, the threshold binding energy (and, accordingly, retention strength in graphite) of the <sup>14</sup>C radionuclide (or its compounds), formed from purging nitrogen and retained in the near-surface layers of the pore structure, is higher in block graphite, than in bushing graphite. This assumption also explains to some extent why there is no proportionality between <sup>14</sup>C and <sup>36</sup>Cl in terms of the leaching rate

for bushing and block graphite. The difference is ~10–15 times for <sup>14</sup>C and ~3–5 times for <sup>36</sup>Cl. The lower values for <sup>36</sup>Cl are explained by the fact that <sup>36</sup>Cl is formed from <sup>35</sup>Cl atoms present initially in the local structural formations of graphite, and is not retained in its structure throughout the surface area of open pores during the operation of the reactor (which is typical of a significant fraction of <sup>14</sup>C). In this case, the accumulation, distribution, and retention of <sup>36</sup>Cl in graphite is largely determined:

- either by the initial distribution of impurity parent atoms in the form of local formations, accumulated during the manufacturing process of graphite blocks,
- or by more complex processes that contribute to the formation of local areas to accumulate <sup>36</sup>Cl atoms during the operation of the reactor.

Another possible reason why there may be differences in the leaching rate of <sup>14</sup>C and <sup>36</sup>Cl between these brands of graphite is that at lower irradiation temperatures these radionuclides can be in physicochemical forms, which most intensely form water-soluble compounds upon contact with aquatic environment. At higher irradiation temperatures, these compounds may not be formed, decompose, or transform into more stable forms.

In the third series, experiments were also performed on the leaching of <sup>14</sup>C and <sup>36</sup>Cl from GR-280 graphite RAW in the form of chips taken away from a container at the site of Leningrad nuclear power plant (LNPP). This type of waste is formed at power units equipped with RBMK-1000 reactors during mechanical processing of graphite blocks to extend the operation life of graphite

**Table 2.** Characteristics of samples of irradiated graphite chips for leaching tests

| Sample | Part, graphite brand     | Kind of sample, weight, g | Irradiation time, year, and temperature, °C | Specific activity of $^{14}\text{C}$ , Bq/g | Specific activity of $^{36}\text{Cl}$ , Bq/g |
|--------|--------------------------|---------------------------|---|---|--|
| Type 4 | Blocks from LNPP, GR-280 | ground graphite, 0.95 g   | (40, 300–700) <sup>a</sup>                  | $7 \times 10^5$                             | $5 \times 10^2$                              |

<sup>a</sup> The temperature range is given for the whole volume of blocks of RBMK graphite masonry in the core area, the irradiation time is taken to be equal to the reactor operation life until the container is filled.

**Table 3.** Fraction of  $^{14}\text{C}$  and  $^{36}\text{Cl}$  released from the graphite sample per unit time ( $\gamma$ ) and the efficient leaching rate for these isotopes  $R_{\text{eff}}$  at the time after 1.5-year of exposure in the leaching fluid (distilled water)

| No. | Graphite brand | $\gamma$ ( $^{14}\text{C}$ ), day <sup>-1</sup> | $\gamma$ ( $^{36}\text{Cl}$ ), day <sup>-1</sup> | $R_{\text{eff}}(^{14}\text{C})$ , g/cm <sup>2</sup> day | $R_{\text{eff}}(^{36}\text{Cl})$ , g/cm <sup>2</sup> day |
|-----|----------------|---|--|---|--|
| 1   | GR-76          | $2 \times 10^{-8}$                              | $3 \times 10^{-5}$                               | $1.7 \times 10^{-10}$                                   | $2.6 \times 10^{-7}$                                     |
| 2   | GR-220         | $2 \times 10^{-9}$                              | $9 \times 10^{-6}$                               | $1.7 \times 10^{-11}$                                   | $7.8 \times 10^{-8}$                                     |
| 3   | GR-280         | $4 \times 10^{-9}$                              | $5 \times 10^{-6}$                               | $3.5 \times 10^{-11\text{a}}$                           | $4.4 \times 10^{-8\text{a}}$                             |

<sup>a</sup> The porosity characteristics for the irradiated GR-280 graphite are taken the same as for the irradiated GR-220 graphite.

masonry. Graphite chips, most likely, is a mixture of material from different graphite blocks, the composition is formed by multiple mixing at stages of cutting, removal of chips from masonry, transportation, and packing into a container.

Leaching tests were performed with two samples of crushed graphite RAW, each 0.95-g weight (Table 2).

Due to the uncertainty in estimation of the effective leaching surface area, the dynamics of fraction of a radionuclide leached per unit time,  $\gamma_n^i(t)$ , was determined during the tests [Eq. (7)]. The dependences of  $\gamma_n^i$  on time for leaching of  $^{14}\text{C}$  and  $^{36}\text{Cl}$  from the samples of crushed block graphite of GR-280 brand from LNPP are demonstrated in Fig. 5. The dependences for monolithic samples of GR-220 block graphite are given for comparison.

The difference in the  $\gamma_n^i$  curves between the samples of these brands is insignificant both for  $^{14}\text{C}$  and  $^{36}\text{Cl}$  (Fig. 5). Graphite samples of the studied brands are similar in production technology, structural characteristics, physical and mechanical properties, isotopic composition, and specific activity, as well as in conditions and duration of irradiation. Nevertheless, the total surface area of crushed graphite particles should be significantly higher than that of non-crushed sample of comparable weight (~0.95 and ~0.85 g, respectively, as in our experiment).

In the given case, insignificant differences in the  $\gamma_n^i(t)$  value for monolithic and crushed samples can be explained by the fact that for graphite crushed to particle sizes typical of those formed by mechanical processing on the equipment used at LNPP the condition  $F_S \gg F_0$  is also valid. Only in this case, crushing of graphite RAW does not lead to a significant change in the effective leaching surface and, accordingly,  $R_{\text{eff}}^i(t)$  and  $\gamma_n^i(t)$  (Fig. 5).

Thus, it is most likely that in this case, the condition  $F_S \gg F_0$  is met even for crushing graphite. In addition, crushing causes material disintegrate predominantly along the surfaces (boundaries) of structural cavities (pores, crystallite boundaries), which in the monolithic sample, as in the crushed one, were also accessible for contact with the solution.

**Recommendations for performing predictive assessments of the release of long-lived radionuclides  $^{14}\text{C}$  and  $^{36}\text{Cl}$  due to the leaching processes under disposal of graphite RAW.** Summarizing all the results on study of the pore structure of graphite samples of domestic brands [9] and the results of this study on the resistance to leaching of radionuclides  $^{14}\text{C}$  and  $^{36}\text{Cl}$  (Figs. 2–5), we can explicitly estimate the effective leaching rate  $R_{\text{eff}}^i$  for these radionuclides [Eq. (6)]. The results of evaluating this parameter after about 1.5-year of exposure in a leaching medium (distilled water) are given in Table 3.

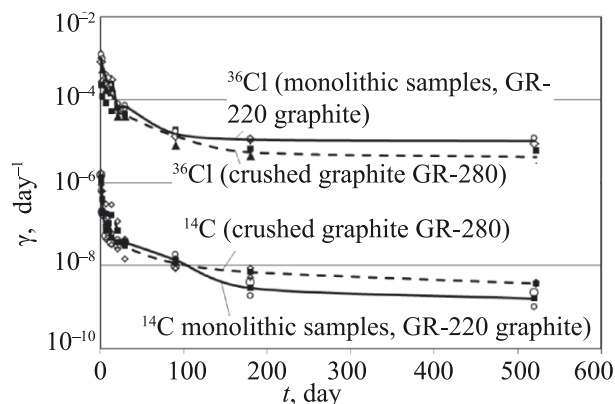


Fig. 5. Dependence of  $\gamma_n^i$  on the time  $t$  for leaching of  $^{14}\text{C}$  and  $^{36}\text{Cl}$  radionuclides from samples of irradiated block graphite.

For monolithic fragments of graphite masonry (blocks, bushings, etc.), the “classical” leaching rate parameter, normalized per unit surface area  $R$  [Eq. (1)] can be also used in practical calculations of the  $^{14}\text{C}$  and  $^{36}\text{Cl}$  migration. In this case however, the  $R$  values obtained on small samples ( $\sim 1\text{ cm}^3$ ) will be incorrect for real large fragments (blocks, bushings) and should be recalculated taking into account their geometry [Eq. (8)]. Experimental  $R$  values obtained on small samples of GR-76 and GR-220 graphite (Fig. 4) and the  $R$  values converted to the “graphite bushing” and “graphite block” geometries are given in Table 4. The geometry of graphite parts from IUGR was chosen as example.

From practical viewpoint, using the fraction of  $^{14}\text{C}$  and  $^{36}\text{Cl}$  released from the graphite RAW per unit time ( $\gamma$ ) as the leaching rate parameter in predictive estimates of radionuclide migration instead of the effective leaching rate  $R_{\text{eff}}$  is preferable, allowing avoidance of labor-consuming determination of the pore structure parameters of graphite samples (pore volume fraction and pore diameter distribution) during the leaching tests.

Table 4. The leaching rate  $R$  of  $^{14}\text{C}$  and  $^{36}\text{Cl}$ , normalized per unit surface area of graphite fragments, at the time after about 1.5-year of exposure in leaching fluid (distilled water) for small samples of GR-76 and GR-220 graphite and the  $R$  values converted to the “graphite bushing” and “graphite block” geometry

| No. | Graphite brand | Geometry of “small sample” ( $\sim 1\text{ cm}^3$ ) |  | Geometry of “real graphite part”                |  |
|-----|----------------|---|--|---|--|
|     |                | $R(^{14}\text{C})$ , $\text{g/cm}^2\text{ day}$     | $R(^{36}\text{Cl})$ , $\text{g/cm}^2\text{ day}$ | $R(^{14}\text{C})$ , $\text{g/cm}^2\text{ day}$ | $R(^{36}\text{Cl})$ , $\text{g/cm}^2\text{ day}$ |
| 1   | GR-76(bushing) | $6 \times 10^{-9}$                                  | $8 \times 10^{-6}$                               | $2.7 \times 10^{-8}$                            | $3.6 \times 10^{-5}$                             |
| 2   | GR-220 (block) | $6 \times 10^{-10}$                                 | $3 \times 10^{-6}$                               | $9 \times 10^{-9}$                              | $4.5 \times 10^{-5}$                             |

The use of  $\gamma$  is most convenient for assessing the dynamics of radionuclide release during leaching when performing predictive calculations of the radionuclide migration to justify the disposal of any masses of graphite RAW, irrespective of geometric configuration of their fragments, in contrast to the use of the “classical” leaching rate parameter normalized to the unit surface area,  $R$ .

In the given case, the release intensity of a radionuclide from the whole mass of disposed graphite RAW (or the mass up to the level of filling with the leaching fluid) will be determined by the equation:

$$a_{\Sigma}^i(t) = \gamma^i(t)MA^i = \gamma^i(t)A_{\Sigma}^i, \quad (9)$$

where  $a_{\Sigma}^i(t)$  is the activity of  $i$ th radionuclide released during leaching per unit time from the whole mass of graphite (or the mass up to the level of filling with the leaching fluid) at time  $t$ , Bq/day;  $\gamma^i(t)$  is a fraction of  $i$ th radionuclide released during leaching per unit time from the whole mass of graphite (or the mass up to the level of filling with the leaching medium) at time  $t$ ,  $\text{day}^{-1}$ ;  $A^i$  is average specific activity of  $i$ th radionuclide in graphite, Bq/g;  $M$  is the total mass of disposed graphite RAW (or the mass up to the level of filling with the leaching fluid), g;  $A_{\Sigma}^i$  is the total activity of  $i$ th radionuclide in the whole mass of disposed graphite RAW (or the mass up to the level of filling with a leaching medium), Bq.

It should be emphasized that Eq. (9) is valid in the period after the leaching process is stabilized, that is:

– all accessible cavities in the graphite structure (spaces between individual fragments, pores, intergranular spaces, etc.) are filled with a leaching medium throughout the whole mass (or up to a certain level) of the graphite RAW and, consequently, the effective leaching surface area is stabilized;



– the intensity of sorption / desorption of radionuclides in the course of their migration towards the boundary of the outer surface of the waste disposal site attained equilibrium.

### CONCLUSION

The structural features of graphite RAW and the operation conditions of UGR largely determine the retention strength and the effective area of a possible contact with the leaching medium of the mobile long-lived radionuclides  $^{14}\text{C}$  and  $^{36}\text{Cl}$  present in irradiated graphite.

In the course of the study, it was determined that almost the whole volume of open porosity in graphite of the studied brands is accessible for saturation with water during exposure. In this case, open pores form a developed three-dimensional network of interconnected channels throughout the graphite volume. The surface area of open pores for graphite of the studied brands, even in the case of small graphite volumes, significantly (more than 2 orders of magnitude) exceeds the surface area of graphite fragments. Owing to these features, the process of leaching of the main volumetrically distributed long-lived radionuclides has close to a “volume” character. A mechanism describing the leaching process, taking into account graphite porosity, is proposed. Parameters numerically characterizing graphite RAW in terms of leaching resistance, independent of geometric shape of individual fragments (samples) are also introduced:  $\gamma_n^i$  is fraction of  $i$ th radionuclide that passed from the material of a sample per unit time during the  $n$ th leaching period, day, and  $R_{\text{eff}}^i$  is the efficient leaching rate of  $i$ th radionuclide, normalized to the effective leaching surface (to take into account the surface area of open pores),  $\text{g}/\text{cm}^2$  day.

These parameters can be recommended for predictive calculations of the long-term dynamics of radionuclide release during leaching from graphite RAW for any projected variant of long-term storage/disposal, irrespective of waste type and amount.

The results of experimental studies on samples of real irradiated graphite from masonry of uranium-graphite reactors testify to the correctness of the proposed mechanism of leaching of the  $^{14}\text{C}$  and  $^{36}\text{Cl}$  radionuclides and the introduction of the above parameters. In the course of experimental study, the main parameters characterizing the resistance to leaching of  $^{14}\text{C}$  and  $^{36}\text{Cl}$  and dynamics of the leaching process during up to

1.5-year period were determined for the main brands of graphite used in the Russian Federation. The influence of the geometric factor owing to the volume character of the leaching process, caused by the pore structure of graphite, is shown. Differences in the resistance to leaching of these radionuclides for graphite parts irradiated under different conditions were experimentally determined. The reason for these differences is most likely due to the irradiation temperature, which determines the features of retention of  $^{14}\text{C}$  and  $^{36}\text{Cl}$  isotopes and their forms in graphite during irradiation.

It should also be noted that in practice, “traditional” leaching rate parameter  $R$  [Eq. (1)], normalized to the unit surface area of the graphite fragment, can be also used in predictive estimate of the  $^{14}\text{C}$  and  $^{36}\text{Cl}$  migration for graphite RAW in the form of solid monolithic articles (blocks, bushings, etc.) or their fragments. It should be kept in mind that this parameter, owing to the “volume” character of the leaching process, depends on the geometry of a particular graphite fragment (article) and, therefore, the  $R$  values obtained for test samples should be recalculated allowing for the geometry of real graphite RAW [Eq. (8)].

From a practical point of view, when predicting the migration of  $^{14}\text{C}$  and  $^{36}\text{Cl}$  for any form of graphite radioactive waste (whole fragments, parts, graphite chips), it is more appropriate to use  $\gamma$  as a parameter characterizing the resistance to leaching of graphite with respect to  $^{14}\text{C}$  and  $^{36}\text{Cl}$ . Contrary to  $R_{\text{eff}}$ , the use of  $\gamma$  allows avoidance of a labor-consuming determination of the pore structure parameters of graphite samples (a fraction of the volume of pores and distribution of pores over diameter) during leaching tests. In addition, the use of this parameter makes it possible to ignore the geometric characteristics of fragments of disposed graphite radioactive waste in calculations.

### FUNDING

The activity of  $^{14}\text{C}$  and  $^{36}\text{Cl}$  radionuclides in the samples was measured on an equipment of the Center for the Collective Use of Physical Research Methods of the Frumkin Institute of Physical Chemistry and Electrochemistry, Russian Academy of Sciences (CCU PMI IPCE RAS). The study was supported in part by the Program no. 14P of the Presidium of the Russian Academy of Sciences.

### CONFLICT OF INTEREST

The authors declare that they have no conflict of interest.

## REFERENCES

- Dorofeev, A.N., Komarov, E.A., Zakharova, E.V., Volkova, A.G., Martynov, K.V., Linge, I.I., Ivanov, A.Yu., Utkin, S.S., Pavlyuk, A.O., and Kotlyarevskii, S.G., *Radioaktivnye Otkhody*, 2019, no. 2(7), p. 18.  
<https://doi.org/10.25283/2587-9707-2019-2-18-30>.
- IAEA TECDOC no. 1790 "Processing of Irradiated Graphite to Meet Acceptance Criteria for Waste Disposal. Results of a Coordinated Research Project," Vienna: IAEA, 2016.
- Pavliuk, A., Bepal, E., and Kotlyarevskiy, S., *ECED 2017 Conference Guide and Book of Abstracts. Eastern and Central European Decommissioning*, June 20–22, 2017, Trnava, Slovakia.
- Tsyganov, A.A., Komarov, E.A., Kotlyarevskiy, S.G., and Pavliyuk A.O., *Bull. Tomsk Polytech. Univ.*, 2007, no. 2, p. 88.
- Wickham, A., Steinmetz, H.-J., O'Sullivan, P., and Ojovan, M.I., *J. Environ. Radioact.*, 2017, vol. 171, pp. 34–40.  
<https://doi.org/10.1016/j.jenvrad.2017.01.022>.
- Bushuev, A.V., Kozhin, A.F., Petrova, E.V., et al., *Radioaktivnyi reaktornyi grafit (Radioactive Reactor Graphite)*, Moscow: MIFI, 2015.
- GOST (State Standard) 29114-91. *Radioactive Waste. Long-time Leaching Measurement of Solidified Radioactive Waste*.
- GOST (State Standard) 52126–2003. *Radioactive Waste. Long-time Leach Testing of Solidified Radioactive Waste Forms*.
- Pavlyuk, A.O., Kotlyarevskii, S.G., Kan, R.I., Volkova, A.G., Zolotov, D.A., Pakhnevich, A.V., Zakharova, E.V., and Shiryaev, A.A., *Radiochemistry*, 2020, vol. 62, no. 6, pp. 526–535.  
<https://doi.org/10.1134/S1066362220060089>
- Pavlyuk, A.O., Kotlyarevskii, S.G., Bepala, E.V., Volkova, A.G., and Zakharova, E.V., *Izv. Tomsk. Politekhn. Univ., Inzhiniring Georesursov*, 2017, no. 328(8), pp. 24–32.
- Bepala, E.V., Pavlyuk, A.O., Zagumenov, V.S., and Kotlyarevskii, S.G., *Izv. Vyssh. Uchebn. Zaved. Yadern. Energetika*, 2017, no. 4, pp. 116–126.  
<https://doi.org/10.26583/npe.2017.4.11>
- Shiryaev, A.A., Volkova, A.G., Zakharova, E.V., et al., *Radiochemistry*, 2018, vol. 60, no. 6, pp. 564–570.  
<https://doi.org/10.1134/S0033831118060151>
- Vukovic, F., Leyssale, J.-M., Aurel, P., and Marks, N.A., *Phys. Rev. Applied.*, 2018, vol. 10, no. 6, ID 064040.  
<https://doi.org/10.1103/PhysRevApplied.10.064040>
- Gurovich, B.A., and Prikhodko, K.E., *RADIAT EFF DEFECTS*, 2001, vol. 154, no. 1, pp. 39–60.  
<https://doi.org/10.1080/10420150108214042>
- Bepala, E.V., Pavlyuk, A.O., Kotlyarevskii, S.G., and Novoselov, I.Yu., *Poverkhnost'. Rentgenovskie, Sinkhrotronnye i Neitronnye Issledovaniya*, 2020, no. 2, pp. 1–9.
- Pokhitonov, Yu.A., *Radiochemistry*, 2020, vol. 62, no. 3, pp. 183–194.  
<https://doi.org/10.1134/S1066362220030017>